



CHALMERS
UNIVERSITY OF TECHNOLOGY

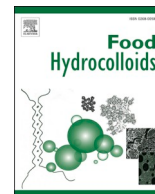
Self-assembly properties of enzymatically treated oat oil

Downloaded from: <https://research.chalmers.se>, 2025-06-08 01:05 UTC

Citation for the original published paper (version of record):

Gladkauskas, E., Gilbert, J., Humphreys, B. et al (2025). Self-assembly properties of enzymatically treated oat oil. *Food Hydrocolloids*, 167. <http://dx.doi.org/10.1016/j.foodhyd.2025.111378>

N.B. When citing this work, cite the original published paper.



Self-assembly properties of enzymatically treated oat oil

Eimantas Gladkauskas^{a,1,*}, Jennifer Gilbert^{b,c,d,e,1}, Ben Humphreys^{c,f}, Scott Montalvo Diaz^a, Anna Maria Piña Cañaveras^a, Ann Terry^g, Jenny Lindberg Yilmaz^{a,h}, Tommy Nylander^{c,d,i,j}, Patrick Adlercreutz^a, Cecilia Tullberg^a

^a Department of Chemistry, Division of Biotechnology, Lund University, Skåne, 223 62, Lund, Sweden

^b Department of Life Sciences, Division of Chemical Biology, Chalmers University of Technology, Kemigården 1, Västra Götaland, 412 58, Gothenburg, Sweden

^c Department of Chemistry, Physical Chemistry, Lund University, Lund, Sweden

^d NanoLund, Lund University, Lund, Sweden

^e NanoLund, Lund University, Professorsgatan 1, Skåne, 223 62, Lund, Sweden

^f Institut Laue-Langevin, 71 Avenue des Martyrs, CS20156, 38042, Grenoble, France

^g MAX IV Laboratory, Lund University, P.O. Box 118, 221 00, Lund, Sweden

^h Department of Experimental Medical Science, Brain Repair and Imaging in Neural Systems (BRAINS) Unit, Lund University, Klinikgatan 32, Skåne, Lund, 221 84, Sweden

ⁱ LINXS Institute of Advanced Neutron and X-Ray Science, Lund, Sweden

^j School of Chemical Engineering and Translational Nanobioscience Research Center, Sungkyunkwan University, Suwon, 16419, Republic of Korea

ARTICLE INFO

Keywords:

Oat oil
Lipolysis
Liquid crystalline phases
Micellar cubic phase
Polar lipids
Triglyceride hydrolysis
Enzymatic modification

ABSTRACT

The enzymatic modification of natural oat oils enriched with polar lipids (PL), consisting mainly of equal mixture of phospholipids and galactolipids, offers a sustainable pathway to produce liquid crystalline phases (LCPs) with diverse structural arrangements, including micellar or bicontinuous cubic and hexagonal phases. These self-assembling lipid systems have potential applications in drug delivery, nutraceuticals, and food formulations due to their ability to encapsulate bioactive compounds, thereby enhancing their stability, and facilitate controlled release.

This study introduces a novel, low-energy, and sustainable one-step enzymatic process that makes oat oil lipids self-assemble into desired types of LCPs without the need for additional surfactants or stabilisers. The polar lipid content was a critical factor in determining the curvature of the lipid-aqueous interface and hence the type of LCP formed. Small angle x-ray scattering (SAXS), cryogenic transmission electron microscopy (cryoTEM), and thin layer chromatography (TLC) was used to elucidate the phase behaviour, structure, and composition of the LCP. Functional additives, such as curcumin, vitamin D, and octyl glucoside (OG), were incorporated into the LCPs with concentrations up to 10 wt%, thereby highlighting the possibility to tailor the system for different applications. Dispersed LCP nanoparticles were successfully produced via sonication and have an internal hexagonal structure as verified by SAXS and cryoTEM. The obtained results show that enzymatic processing using lipolytic enzymes can be used to control the conversion of oat oil with the polar lipid content ranging from 15 to 60 wt% into LCPs with either lamellar, micellar cubic (Fd3m) or reversed hexagonal internal structure.

1. Introduction

There is an increasing interest in incorporating bioactive compounds that are natural and sustainably produced into food, nutraceutical, and pharmaceutical products with lipid based formulations that maintain the stability of the active compounds and promote high bioavailability.

Effective oral delivery systems not only prevent the deterioration of bioactive ingredients, e.g. nutraceuticals and drugs, but also ensure efficient gastrointestinal tract absorption, maximising their therapeutic effects and nutritional benefits (Boyd et al., 2021). Polar lipids were found to be ideal for stabilising formulations due to their amphiphilic nature, which allows them to accommodate both hydrophilic and

This article is part of a special issue entitled: Boosting structural food science published in Food Hydrocolloids.

* Corresponding author.

E-mail address: eimantas.gladkauskas@ple.lth.se (E. Gladkauskas).

¹ These authors contributed equally to this work.

<https://doi.org/10.1016/j.foodhyd.2025.111378>

Received 20 December 2024; Received in revised form 7 March 2025; Accepted 23 March 2025

Available online 25 March 2025

0268-005X/© 2025 The Authors. Published by Elsevier Ltd. This is an open access article under the CC BY license (<http://creativecommons.org/licenses/by/4.0/>).

hydrophobic bioactive substances and act as emulsifiers (Freire & Salentinig, 2024). For example, different oat extracts from oat processing side streams, such as saponins and polar lipids, consisting mainly of phospholipids and galactolipids (Doehlert et al., 2010), were used as natural emulsifiers with a range of industrial applications (Kaimainen et al., 2012; Ralla et al., 2018).

1.1. Self-assembling systems based on polar lipids

Polar lipids can self-assemble into different structures, depending on the lipid composition and environmental conditions. Emulsions are mixtures of two (or more) immiscible liquids, like oil and water, where the dispersion is stabilised by an emulsifier. Common emulsifiers include proteins, carbohydrate derivatives or polar lipids, such as phosphatidylcholine, widely used in food applications (McClements and Jafari, 2018). In oil-in-water (O/W) emulsions, droplets of oil, stabilised by an emulsifier, are suspended in an aqueous medium for which the pressure between the inside and outside of the droplet, ΔP , is determined by the Laplace equation, $\Delta P = 2\gamma/R$, where γ is the interfacial tension and R is the radius of the drop. Hence, to obtain small droplets a low interfacial tension is needed, otherwise the number of large droplets will increase at the expense of the smaller ones. The droplet size of an emulsion is therefore often polydisperse, and ultimately the stability of an emulsion with natural emulsifiers can be compromised leading to phase separation and loss of functionality.

Liquid crystalline phases (LCPs), on the other hand, are ordered structures formed in different solvents through the self-assembly of amphiphilic molecules and can be distinguished by their specific geometrical arrangements (Larsson, 1989; Luzzati & Husson, 1962; Milak and Zimmer, 2015; Ninham et al., 2017). Well-defined lipid-based mixtures, containing components such as glycerol monooleate, phytantriol, glycolipids and phosphatidylcholines, are typically used in applications involving the self-assembly of LCPs (Engstedt et al., 2023; Wang et al., 2023; Barauskas & Landh, 2003; Barauskas & Nylander, 2008, pp. 107–131; Seddon et al., 2000).

LCPs have been extensively investigated for their ability to incorporate various additives in both the lipid domains and aqueous cavities. They have been applied as systems for controlled drug release, where drug interactions and release can be triggered by structural changes in response to environmental factors (Barriga et al., 2019; Costa-Balogh et al., 2010; Rossetti et al., 2011).

Inverse LCPs, where the lipid-aqueous interface is curved towards the aqueous phase, are especially of interest for drug delivery applications, as they form aqueous cavities. The bulk LCPs can be dispersed into an excess aqueous medium with a narrow nanoparticle size distribution, retaining their internal structure (Barauskas et al., 2005; Barriga et al., 2019; Larsson, 2009). The various inverse liquid crystalline phases, such as the reversed bicontinuous cubic (V_2), reversed hexagonal (H_{II}), reversed micellar cubic (I_2), and sponge (L_3) phases represent distinct structural arrangements that provide cavities to enclose bioactive molecules. The reverse micellar or discrete cubic phase, I_2 , features micelles organised in a cubic array with a high symmetry space group, such as $Fd3m$ (Huang et al., 1996). On the other hand, the H_{II} phase, or the inverted hexagonal phase, is characterised by hexagonally packed tubular structures (Ramezanpour et al., 2020).

The LCPs have significant potential for applications in diverse fields, including drug delivery systems, food technology, and cosmetic formulations. However, in most cases, organic solvents are required to facilitate lipid mixing, and the production of pure lipids often involves energy-intensive processes and organic solvents for purification (Meng et al., 2023; Mouloungui et al., 2009), hence natural lipid sources and mild production methods are needed to overcome the latter challenges.

1.2. Natural lipids and bioactives in oat oil

Natural vegetable oils, such as oat oils, are a natural source of lipids

that can be used in the preparation of LCPs. There is an increasing awareness of the necessity to understand and control the bioaccessibility and bioavailability of dietary lipids and how it depends on their organisation (Amara et al., 2024). The interest for using oat oil has increased recently thanks to its particular composition and the health benefits it offers. The abundance of antioxidants, proteins, minerals, lipids, and other beneficial bioactive compounds in oats have been suggested to have the ability to protect the cardiovascular system, as well as possessing anti-obesity and even anti-diabetic properties (Liu et al., 2016; Tang et al., 2022; Wang et al., 2019). Oat oil is furthermore unusually rich in polar lipids, here referred to as an oil fraction rich in phospholipids and galactolipids, with levels of 10 % phospholipids and 11 % glycolipids reported (Doehlert et al., 2010). The glycolipids include several galactolipids, digalactosyldiacylglycerol (DGDG) being the most abundant (Doehlert et al., 2010). Beyond structurally interesting features, DGDG has been connected with beneficial health effects, such as anti-inflammatory properties in *in vitro* studies (De Los Reyes et al., 2016).

Incorporating oat lipids into everyday meals might significantly reduce the glycemic response, triacylglycerol, and ghrelin, while increasing GLP-1 and PYY hormone levels in the blood (Hossain et al., 2023). The broad spectrum of bioactive compounds, numerous health benefits, natural origin, and emulsifying ability, positions oat oils as important plant-based and sustainable raw materials.

1.3. Mild processing of natural lipids

Additional processing of oat oils makes it possible to modify the lipids to tune their properties in terms of self-assembly and surface activity, to produce high-value components, underlining the versatility of this material. Recent advancements in enzymatic processes have opened pathways to modify lipid properties and their self-assembly structure in a more sustainable way (Barchan & Adlercreutz, 2024). This includes using enzymes like lipases to perform hydrolysis and glycerolysis of oils, producing monoacyl- and diacylglycerols (MAGs and DAGs), and free fatty acids (FFAs), components important in self-assembly systems (Fay et al., 2012; Yaghmur et al., 2023; Zheng et al., 2023).

Previous studies have shown that lipase catalysed digestion of monoolein leads to a transition of the structures that follows the monoolein—oleic acid—aqueous ternary phase diagram and is strongly dependent on the pH or the degree of protonation of the fatty acid product (Borné et al., 2002). Hence transitions from cubic \rightarrow reversed hexagonal \rightarrow micellar cubic \rightarrow reversed micellar phase + dispersion occurs with time at low pH, whereas at high pH the sequence of structures follows the monoolein—sodium oleate—aqueous ternary phase diagram. Here, the lamellar phase dominates, which, with time, transitions into a normal hexagonal phase.

Here, we introduce a novel, low-energy, one-step, enzymatic method to produce bulk liquid crystalline phases from oat oils enriched with oat polar lipids. The enzymatic process leads to the hydrolysis of oat oil, creating MAGs, DAGs, and FFAs, which in turn can form liquid crystalline phases with a controllable structure.

In order to establish the relation between the type of LCPs formed and their phase behaviour as well as the influence of the preparation conditions including temperature, oil composition, inclusion of additives and lipase used, we combined small angle x-ray scattering (SAXS), cryogenic transmission electron microscopy (cryoTEM), and thin layer chromatography (TLC). These fundamental insights provided will help us to better understand the self-assembly processes as well as defining potential industrial applications and new processes that are more environmentally sustainable.

2. Experimental

2.1. Materials

2.1.1. Oat oil

Oat oils SWEAT® Oil PL4, PL15, and PL40 were kindly supplied by Swedish Oat Fiber (Bua, Sweden). The oil contained different amounts of polar -and nonpolar lipids, like triacylglycerols, and are known to be especially rich in phospholipids and galactolipids (Doehlert et al., 2010). According to the supplier, the PL4 fraction contains approximately 4 g of polar lipids, and 95 g of nonpolar lipids, while the PL15 sample contains 15 g of polar and 82 g of nonpolar lipids, and PL40 - 40 g of polar and 58 g of nonpolar lipids. When studying the effect of polar lipid content, PL50 and PL60 oat oils were prepared by addition of a concentrated fraction of oat oil DGDG (95 % purity) from Swedish Oat Fiber AB (Bua, Sweden).

2.1.2. Enzymes

The enzymatic preparations Lipozyme® RM (*Rhizomucor miehei*) and Lipozyme® LT (*Thermomyces lanuginosus*) were supplied by Novozymes, now known as Novonesis, Denmark). Both preparations are solutions of free enzymes with sn-1,3 position specificity in triacylglycerol hydrolysis. The activities of the enzymatic preparations were 0.275 and 100 KLU/g respectively for hydrolysis of glycerol tributryate.

2.1.3. Buffer salts

Sodium dihydrogen phosphate monohydrate (Merck, Germany) and disodium hydrogen phosphate dihydrate (Merck, Germany) were used to prepare 0.1 M phosphate buffer. The pH was adjusted to 7 with hydrochloric acid (EMSURE®, Supelco, Sigma-Aldrich, Germany) and sodium hydroxide (Sigma-Aldrich, Germany), using Phenomenal™pH 1000L (VWR International, Germany) pH meter. Ultrapure di-ionised water (Milli-Q IQ 7000, Millipak 0.22 µm, Merck, Germany) was used in all experiments.

2.1.4. Octyl glucoside (OG) and other additives

The effect of including several types of additives into the liquid crystalline phases was tested; Octyl glucoside (OG) 0–10 wt% oil (n-Octyl-β-D-glucopyranoside, ANAGRADE®, Anatrace,USA), Curcumin 10 mg/g oil (Turmeric, powder, Sigma-Aldrich, Germany), Vitamin D 10 µg/ml oil (Ergocalciferol, >98 %, Sigma-Aldrich, Germany), Iron(II) sulphate heptahydrate 83 mg/ml oil (ACS reagent, >99 %, Sigma-Aldrich, Germany), Fish oil capsules (Omega 3, FORTE 70 % EPA and DHA, ICA AB, Sweden) were cut open, and the recovered fish oil was used as an additive at 5 and 10 wt% oil. Water soluble compounds were dissolved in the buffer prior to hydration of the SWEAT® Oil, and water insoluble substances were mixed in the oil phase before hydration.

2.2. Methods

2.2.1. Preparation of bulk liquid crystalline phases

The experiments utilised oat oil that was enriched with a polar lipid fraction derived from oats. For the experiments, 300 mg of polar lipid-enriched oat oil (PLX, where X = 4, 15, 25, 30, 40, 50, 60), which contained 4–60 wt% polar lipids, was combined with 1.2 mL of a 0.1M pH 7 phosphate buffer in 4.5 mL glass sample tubes. This gives a total lipid content of 20 wt%, which is expected to correspond to a fully swollen liquid crystalline phase. Subsequently, for the samples undergoing enzymatic processing, 10 µL of a commercial lipase solution Lipozyme RM or Lipozyme TL (Novozymes, Denmark) was introduced to each sample and briefly vortexed to mix. All samples were then incubated in a thermomixer (Hettich BENELUX, MHR 13) operating at 700 rpm at a temperature of 40 °C (for time T, where T = 6, 12, 16, 24, 48, 96 h). The method has been developed in-house.

After initial investigation of the effect of the amount of PL content, all further investigations were performed using PL40, containing 40 wt

% polar lipids.

2.2.2. Formulation of dispersed liquid crystalline phases

Bulk liquid crystalline phases were prepared as described above, utilising 300 mg of oat oil PL40, which contained 40 % PL wt%, combined with 1.2 mL of 0.1M pH 7 phosphate buffer and 10 µL of lipase solution Lipozyme TL or RM. After incubation (for time T, where T = 2, 6, 24 h), phase separation occurred, and 50 mg of the bulk liquid crystalline phase was collected and subsequently dispersed 1:100 in buffer through tip sonication for 5 min with 1 s pulses at 35 % amplitude (UP400S, 400W 24 kHz, Hielscher, Germany). The method has been developed in-house.

2.2.3. Small angle X-ray scattering

The self-assembly structure of bulk and dispersed samples, prepared as described above, were determined using a SAXSLab Ganesha 300XL (SAXSLAB ApS, Skovlunde, Denmark) with a 2D Pilatus 300K detector (Dectris) and Genix 3D x-ray source (x-ray wavelength $\lambda = 1.54 \text{ \AA}$). The samples were sandwiched between two thin mica windows and placed in a thermostated metal block. The temperature of the sample holder was controlled by an external water bath set to the desired temperature. All samples were investigated with SAXS over the q range: $0.003 \text{ \AA}^{-1} < q < 0.753 \text{ \AA}^{-1}$ with an exposure time of 1 h. The dispersion samples were also characterised in the WAXS range: $0.01 \text{ \AA}^{-1} < q < 2.9 \text{ \AA}^{-1}$ for 15 min. I(q) was obtained by radially averaging the 2D scattering pattern using SAXSGui. The background was manually subtracted and all further analysis was performed using MATLAB R2020b (MathWorks, United States).

Selected dispersion samples were further characterised at the CoSAXS beamline, MAX IV (Lund University, Sweden) using an Eiger2 4M SAXS detector and wavelength of 1 Å. The samples were loaded into a quartz capillary (diameter = 1.5 mm) using an autoloader and measured at room temperature ($25 \text{ °C} \pm 1 \text{ °C}$) over the q range $0.003 \text{ \AA}^{-1} < q < 0.318 \text{ \AA}^{-1}$ (sample to detector distance = 3.044 m, calibrated using silver behenate). For each sample, 300 frames with exposure time of 20 ms were collected, which were integrated, reduced, averaged together and the solvent background subtracted by the CoSAXS autor-eduction pipeline and custom Python Jupyter Notebook scripts (Jensen et al., 2022). All further analysis was performed using MATLAB R2020b (MathWorks, United States).

2.2.4. Calculating lattice parameter

The ratios between the peak positions, q_{peak} , in the SAXS curves were used to identify the liquid crystalline structure and calculate the corresponding lattice parameter (i.e. unit cell dimension). The repeat distance, d_{hkl} , corresponding to the peak q position can be calculated as follows:

$$d_{hkl} = \frac{2\pi}{q_{peak}}$$

The lattice parameter, a, in the figures were calculated as described in Table 1) For lamellar, hexagonal and Fd3m: standard deviation was calculated from 3(+) peaks.

For disordered phases the instrument resolution was used.

2.2.5. DLS

The dispersion samples were diluted 10 times in MilliQ water and loaded into DTS1070 disposable folded capillary cells for DLS measurements, which were performed using a Zetasizer Nano ZS (Malvern Instruments Ltd., United Kingdom). The temperature was set to 25 °C and samples were equilibrated for 60 s before measurement in triplicate. The Stokes-Einstein equation was used to calculate the apparent hydrodynamic diameter with viscosity of water, $\eta = 0.8872 \text{ cP}$ and assuming spherical particles.

Table 1
Conditions for preparation of bulk liquid crystalline phases.

Sample	Lipase name, source, and specificity; activity	Comments	Incubation time, h	Temperature, °C
A	No lipase	0.1M pH 7 phosphate buffer	16	40
B	Lipozyme® RM, <i>Rhizomucor miehei</i> , (Novozymes); sn1,3 directed; 0.275 KLU/g	0.1M pH 7 phosphate buffer	6,12, 16, 24, 48, 96	40
C	Lipozyme® TL, <i>Thermomyces lanuginosus</i> , (Novozymes), sn1,3 directed, 100 KLU/g	0.1M pH 7 phosphate buffer	6, 12, 24, 48	40

2.2.6. CryoTEM

CryoTEM measurements were performed using the same sample preparation and instrument set up as described in Dubackic et al., 2022, at the National Center for High Resolution Electron Microscopy (nCHREM) at Lund University. In summary, samples were diluted 1:2 times in phosphate buffer (0.1 M, pH 7), vortexed for 20 s and tip sonicated for 1 min. 2.6–4 µL of the sample was deposited on a lacey carbon grid and blotted to remove excess liquid. The grid was immediately plunged into liquid ethane (approx. −184 °C) using a Leica EM GP grid plunger (Leica Microsystems GmbH, Germany) and stored in liquid nitrogen (−196 °C) until imaging with a JEM-2200FS transmission electron microscope (JEOL). The internal structures of the particles imaged by cryoTEM were further analysed in ImageJ (Schneider et al., 2012).

2.2.7. Lipid extraction and analysis using high performance thin layer chromatography

Samples for the TLC analysis were prepared by extracting lipids from bulk liquid crystalline phases. The lipid extraction was done by taking 30 mg of the LCP, adding 3.75 mL of chloroform:MeOH (1:1 v/v with 0.05 % BHT w/v), 1 mL 0.15 mM acetic acid, 1.25 mL of chloroform and 1.25 mL of MilliQ water, where vortexing was done for 5 s in between every addition of solvents. The samples were then centrifuged at 595 g for 10 min (Eppendorf® Centrifuge 5910 Ri, Sigma Aldrich, Merck), following by transferring of the lower phase to a separate vial for TLC analysis. The TLC analysis was done using the CAMAG system (CAMAG TLC Scanner 3, CAMAG Automatic TLC Sampler 4). The samples were applied on HPLC Silica gel 60 plate (Merck, Germany). Chamber saturation time was set to 20 min, volume front trough was 20 mL, volume rear trough was 40 mL, and drying time was set to 5 min. Chamber development was done at room temperature. Plate spraying was done using 0.05 % primulin in acetone:water (8:2 v/v) solution and lipids were visualised under UV light.

3. Results and discussion

3.1. Bulk liquid crystalline phases - structure and composition

The structure of formed LCPs controls the physicochemical properties of the system and hence is crucial for different potential application. SAXS was employed to examine the lipid liquid crystal structures of the samples formed under different conditions. This analysis covered a comprehensive range of polar lipid contents, temperatures and included model additives, such as bioactive components as well as dispersants. The effect on the structural characteristics of the final formulation provided insights that are essential for optimising LCP-based products.

The initial study included the effect of different amounts of polar lipids in the oat oil mixtures, different lipases used in the enzymatic processing step and the enzyme incubation time. After optimisation of

the standard formulation, the effect of temperature and encapsulation of relevant nutraceutical additives on the self-assembled structure of this formulation was investigated.

3.1.1. Polar lipid content

After the enzymatic processing, all bulk samples appeared as white to light brown opaque, stiff gels in excess water, indicating they were at maximum hydration. As shown in Fig. 1A, at 4 % polar lipid in the oat oil, the emulsion had a lamellar (L_{α}) structure, as indicated by the peaks present that occur at 1:2:3 in q ratio in the SAXS data. The L_{α} phase coexists alongside a disordered structure up to 25 % polar lipid, at which a transition to a micellar cubic phase with the Fd3m space group occurs (Fd3m, peak ratio: $\sqrt{3}, \sqrt{8}, \sqrt{11}, \sqrt{12}, \sqrt{16}$, etc.) at 30 % polar lipids. At 50 % polar lipids, mixed micellar cubic, I_2 and H_{II} phases are present, which transforms into a pure H_{II} at 60 % PL.

From the data, a general trend can be observed in which the sample tends to form structures with increasing curvature, from L_{α} to I_2 phase, as the polar lipid content of the oat oil increases. At the highest polar lipid proportion, however, a transition from I_2 to H_{II} is observed, which was not expected. Although the I_2 and H phases are very closely structurally related, as there is a small energy cost associated with transitioning from the fcc-packed spheres of Fd3m space group in the I_2 to the hexagonally packed tubes of H_{II} , the phase sequence usually follows $H_{II} \rightarrow I_2 \rightarrow L_2$ (reverse micelles) (Yagmur & Rappolt, 2013). The reason for the observed phase sequence here remains unclear, but is most likely linked to the complex mixture of lipids in the system. Oat oil contains a variety of both phospholipids and galactolipids, which can be assumed to influence the phase behaviour.

It was also observed that the lattice parameter of the I_2 and H_{II} structures increased with increasing polar lipid content as illustrated in Fig. 1B. The lattice parameter of the lamellar samples remained constant, but the relative contribution, as judged from the peak intensity, of the lamellar structure decreased and the disordered structure increased with increasing polar lipids. For all subsequent experiments, a polar lipid content of 40 % (PL40) was selected.

3.1.2. Lipozyme RM and TL comparison

The differences between the two lipases Lipozyme RM and TL in terms of activity and the structural evolution of the lipid phases during hydrolysis of oat oil containing 40 % polar lipid (PL40) was compared. Both the RM and TL enzymes target the sn-1,3 positions on the glycerol backbone, hence the same hydrolysis reaction is catalysed and it would be expected that the same liquid crystalline phases are formed albeit with different rates.

As shown in Fig. 1C and D, a notable difference was observed in the time point at which Fd3m phase was observed. The Lipozyme TL induced a fully formed I_2 phase with Fd3m space group (hereafter referred to as Fd3m) after 6 h of incubation, whereas Lipozyme RM required 16 h of incubation to achieve the same phase transition. This indicates that the Lipozyme TL facilitates a faster hydrolysis of the TAGs, compared to RM. This agrees with the higher activity of Lipozyme TL on the standard substrate glycerol tributyrates (Table 2. Although the hydrolysis of oat oil involves the hydrolysis of triacylglycerols with much longer chain length, it is likely that Lipozyme TL has a higher catalytic activity than Lipozyme RM also on this type of substrate.

Further analysis of the end point of the reaction Fig. 1E, revealed that both Lipozyme RM and TL preparations resulted in the formation of the same final Fd3m space group, with nearly identical lattice parameters. The outcome was consistent across both enzymes, confirming that the certain level of hydrolysis of TAG (and most probably the ratios between DAG, MAG and fatty acids) must be reached for the same liquid crystalline phase to form, regardless of the lipase used. The different activities of Lipozyme RM and TL on the acyl glycerols of oat oil were most likely the reason for the difference in required incubation time.

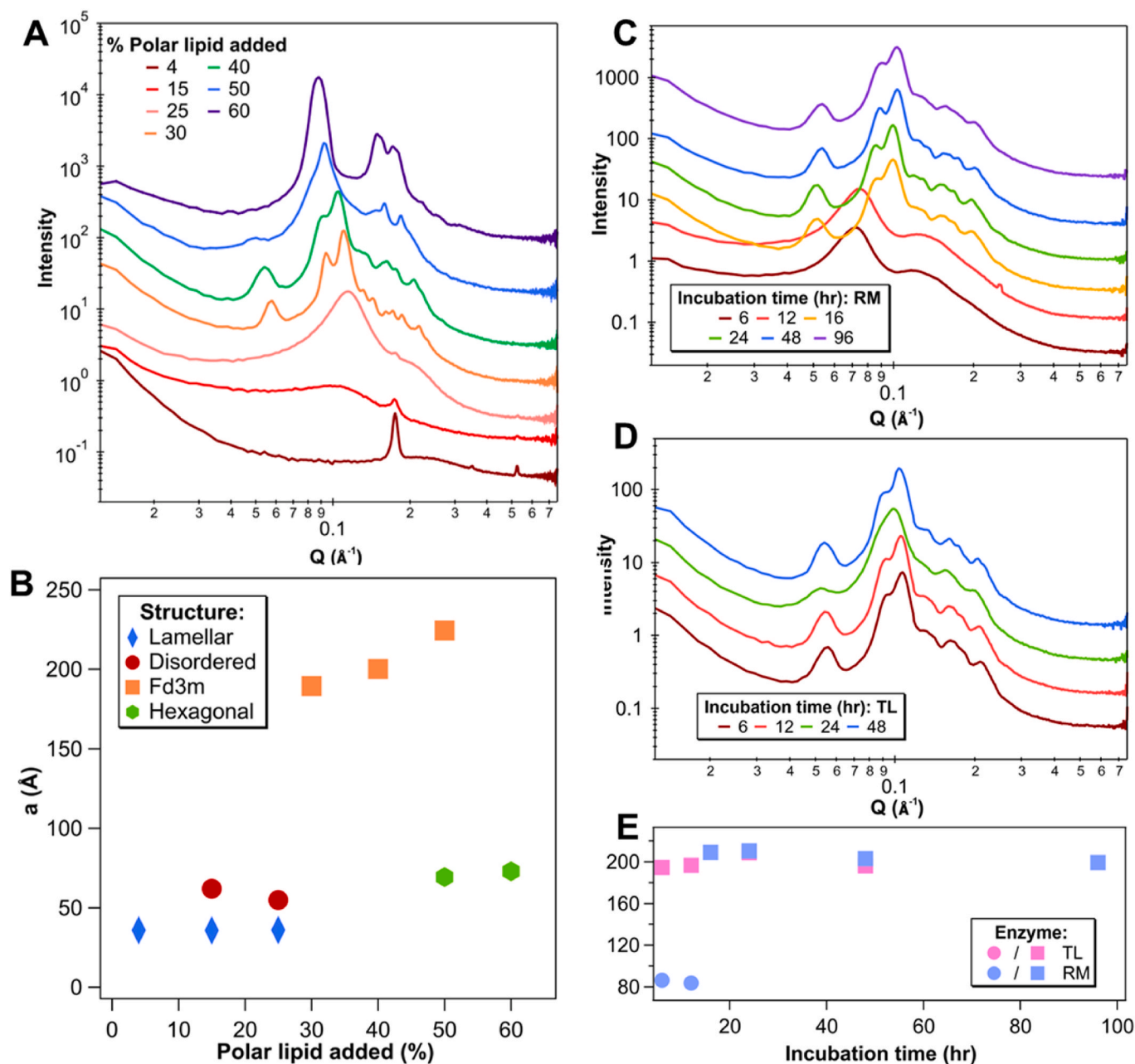


Fig. 1. SAXS data collected from bulk samples prepared using different polar lipid content, type of lipolytic enzyme and incubation time. The total lipid content of 20 wt%, is expected to correspond to a fully swollen liquid crystalline phases. The lipid liquid crystalline structure was indexed and the corresponding lattice parameters were calculated from the SAXS data as specified in the methods section. SAXS data (A) and the corresponding lattice parameters (B) for samples with different proportions of polar lipids (after incubation for 16 h with Lipzyme RM) are shown. The results indicate that increasing the polar lipid content resulted in the formation of structures with higher lipid-aqueous interfacial curvature. SAXS data for PL40 samples incubated with the enzymes Lipzyme RM (C) and TL (D) over different time periods show that the same final structure is formed with the same lattice parameter (E). For the calculated lattice parameters, the structures are indicated by the marker shape (disordered = circle, Fd3m micellar cubic = square, lamellar = diamond, hexagonal = hexagon). All SAXS curves are offset for clarity. Error bars are plotted for all points in B and E. If not visible, they are within the size of the marker.

3.1.3. Evolution of structure with enzymatic hydrolysis incubation time

The evolution of the bulk phase structure with incubation time of PL40 oat oil with Lipzyme RM, representing different extents of hydrolysis, is shown in Fig. 1C. Initially, a disordered structure was observed (indicated by a broad peak), which could possibly indicate the formation of a bicontinuous structure. As the incubation time and hydrolysis of TAG progresses (converting TAG to DAG, MAG and FFAs), a transition to the Fd3m phase becomes evident after 16 h of enzymatic incubation. This indicates an increasing curvature of the lipid-aqueous interface and, as defined Bragg peaks occur, an increase of order within

the system. The data suggests that once the Fd3m phase is formed, longer incubation times do not have an effect on the structures formed. This could indicate that once the LCP is formed, lipases have limited access to the remaining DAG and MAG substrate molecules and the system approaches steady state in terms of hydrolysis.

The hydrolysis of TAG to DAG and MAG introduces a greater proportion of titratable components, such as FFAs, for which the degree of protonation affects the curvature towards the water phase. While TAG hydrolysis towards MAG typically results in a lower curvature towards the water phase, the curvature can still be highly influenced by the

Table 2

The liquid crystalline phases identified in these samples including the equations used to determine the lattice parameter (unit cell dimension) and the characteristic ratios between the peak positions in SAXS.

Liquid crystalline structure	Lattice parameter	Ratio between peak positions
Lamellar $L\alpha$ ($h = k = 0$)	$a_{L\alpha} = ld_i$	$l=1, 2, 3, 4, 5, 6 \dots$
Hexagonal H ($l = 0$)	$a_H = \frac{2\sqrt{(h^2 + k^2 + hk^2)} d_{hkl}}{\sqrt{3}}$	$\sqrt{(h^2 + k^2 + hk^2)} = 1, \sqrt{3}, 2, \sqrt{7}, 3, \sqrt{12} \dots$
Micellar cubic with space group Fd3m	$a_{Fd3m} = \frac{(\sqrt{h^2 + k^2 + l^2} d_{hkl})}{(\sqrt{h^2 + k^2 + l^2})}$	$(\sqrt{h^2 + k^2 + l^2}) = \sqrt{3}, \sqrt{8}, \sqrt{11}, \sqrt{12}, \sqrt{16}, \sqrt{19}, \sqrt{24}, \sqrt{27}, \sqrt{32}, \sqrt{44} \dots$
Disordered	$a = d_{dis} = \frac{2\pi}{q_{first\ peak}}$	-

environmental conditions such as pH and ionic strength. This is particularly true for FFAs (e.g., oleic acid) (Mele et al., 2018) where the phase behaviour is complex and depends on the proportion of protonated and charged FFAs. MAGs (e.g., monoolein) (Kulkarni et al., 2011) also exhibit rich phase behaviour that is highly dependent on factors such as chain length, saturation, and other components in the mixture. The results presented in Fig. 1C are expected, and the presence of key components in the bulk phases, crucial for self-assembly, is confirmed through the TLC analysis discussed below and shown in Fig. 2.

3.1.4. Composition analysis of standard conditions

In order to better understand the main components that are present in the LCPs once they have formed, bulk LCPs formed from enzymatically modified oat oil enriched with 4–40 % polar lipids were analysed using TLC. For this, LCPs were prepared in triplicates, the lipids were extracted and analysed by spotting on the TLC-plate. When comparing the enzymatically treated and untreated oils and LCPs, as seen in Fig. 2, the main groups of lipids that were identified in enzymatically treated oat oils and LCPs were FFAs, and polar lipids, with low levels of MAGs and DAGs. The TAG levels were observed to decrease considerably after 16 h enzymatic treatment, compared to the untreated oat oil.

The TLC results were expected based on the known activity of the enzyme Lipozyme RM that was used during the treatment of the oat oil. The enzyme is specific for the sn-1,3 positions of TAGs, preferentially hydrolysing the fatty acids in the outer positions when water is present. This results in the formation of DAGs and MAGs, along with the release of FFAs. The polar lipids present in the oil samples were assumed not to be altered by the enzymatic modification due to the enzyme specificity.

3.1.5. Effect of temperature (Lipozyme RM)

The stability of the structures of the bulk phases formed from oat oil containing 40 wt% PL (PL40), after 12, 24 and 96 h incubation with the Lipozyme RM, was studied with respect to temperature.

After 12 h of incubation, the bulk phase exhibited a disordered structure, as indicated by the presence of two broad peaks in the SAXS data, Fig. 3A. Upon increasing the temperature, these peaks shifted to higher q-values, corresponding to a decrease in lattice parameter by approximately 20 Å across the entire temperature range. The structure

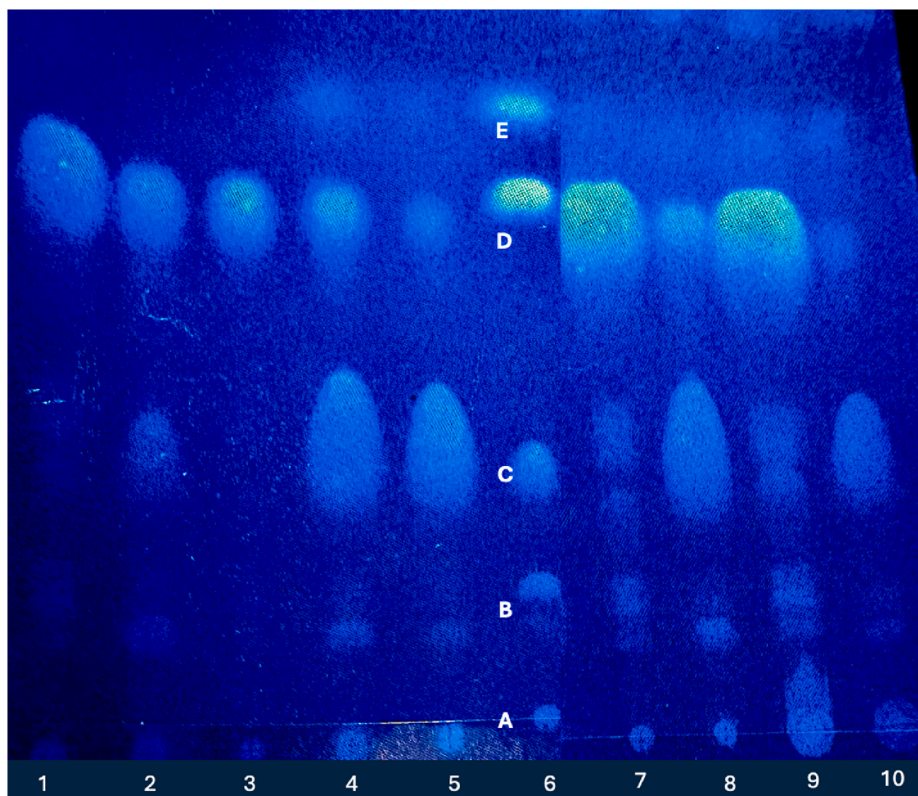


Fig. 2. The composition of the studied samples as obtained from thin layer chromatogram (TLC) of enzymatically treated (2h and 16h) and untreated oat oil enriched with polar lipids. 1–15 wt% polar lipids (PL15) oat oil reference (no enzymatic treatment). 2 – 15 wt% polar lipids (PL15) oat oil after 2h treatment with Lipozyme RM. 3 – 15 wt% polar lipids (PL15) oat oil after 2h reference without enzyme (control). 4 – 15 wt% polar lipids (PL15) oat oil after 16h of Lipozyme RM treatment. 5 – 15 wt% polar lipids (PL15) oat oil with 10 % wt% OG, after 16h of Lipozyme RM treatment. 6 - lipid standards. 7 - Oat oil with 4 wt% polar lipids (PL4) reference (no enzymatic treatment). 8 - Oat oil with 4 wt% polar lipids (PL4) after 16h of Lipozyme RM treatment. 9 - Oat oil with 40 wt% polar lipids (PL40) reference (no enzymatic treatment). 10 - Oat oil with 40 wt% polar lipids (PL40) after 16h of Lipozyme RM treatment.: A – Standard with monoacylglycerols (MAGs) and polar lipids (PL), B - DAGs – diacylglycerols (DAGs), C - free fatty acids (FFAs), D – triacylglycerols (TAGs), E - fatty acid methyl esters (FAME). It should be noted that the image has been cropped to show only the sample discussed here. Only the relevant data for this publication is visible in the current image.

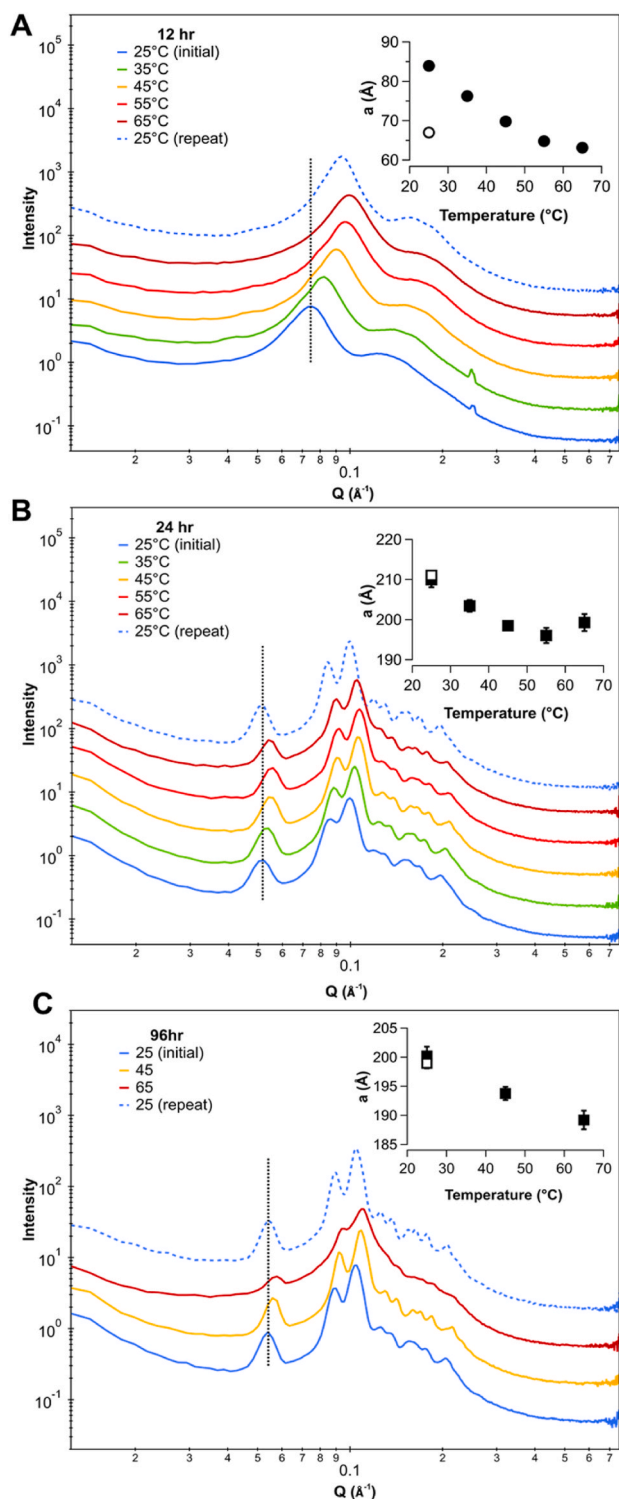


Fig. 3. SAXS data for bulk samples made with oat oil containing 40 wt% polar lipids (PL40). The samples were incubated with Lipozyme RM for 12 h (A), 24 h (B) or 96 h (C) heated from 25 °C up to 65 °C and then after returning to 25 °C. The total lipid content of 20 wt%, is expected to correspond to a fully swollen liquid crystalline phase. The dashed vertical line indicates the position of the lowest q peak from the initial measurement at 25 °C and the inset for each figure shows the change in calculated lattice parameter with temperature. For the calculated lattice parameters, the structures are indicated by the marker shape (disordered phase = circle, Fd3m micellar cubic = square) and initial and final measurements at 25 °C are indicated by filled and empty markers respectively. All SAXS curves are offset for clarity. Error bars are plotted for all points in the inset figures. If not visible, they are within the size of the marker.

only partially recovered when cooled back to 25 °C, with the lattice parameter remaining smaller than the initial measurement at 25 °C. Additionally, a small, sharp peak observed at $\sim 0.25 \text{ \AA}^{-1}$ in the SAXS data at 25 °C and 35 °C, possibly indicative of a crystalline structure, was found to melt at 45 °C and did not reappear upon cooling.

In contrast, for longer enzymatic incubation times of 24 and 96 h, the Fd3m micellar cubic phase that formed after the lipolysis reaction exhibited greater thermal stability. After cycling the temperature back to 25 °C, the Fd3m phase fully recovered, and the change in peak position with increasing temperature was less pronounced compared to the disordered phase observed at shorter incubation times.

An overall decrease in lattice parameter was observed with increasing temperature independent of the enzymatic incubation times, (as shown in the insets of Fig. 3A–C). This behaviour can be attributed to the increase in hydrophobic volume and dehydration of the polar regions, which, in the case of an inverse structure (i.e., curving towards the water phase), leads to a reduction in the diameter of the water compartments. Interestingly, the Fd3m phase appears to be less responsive to temperature changes than expected, as seen in Fig. 3B and C. Typically, a transition to a less ordered phase, such as L_2 , would be anticipated with increasing temperature. The observed stability of the Fd3m phase verified that the observed micellar cubic phase structure was of the inverse type. In this case, where oil is the continuous phase, an increase in temperature could potentially reduce packing frustration, contributing to the observed thermal stability.

3.1.6. Effect of additives

Different additives and their effects on the enzyme catalysed hydrolysis and self-assembly of the liquid crystalline structures were tested. In particular, curcumin, vitamin D, fish oil at different concentrations, iron sulphate and different concentrations of OG were investigated for the standard formulation of 40 % polar lipid oat oil (PL40) incubated with Lipozyme RM for 24 h. Particular emphasis was placed on the effects of OG, a non-ionic surfactant known for its ability to modulate properties of lipid membranes (Misquitta & Caffrey, 2003). In their work, Misquitta and Caffrey used OG to influence the phase behaviour of a monoolein (MAG) bicontinuous cubic phase, which is often used for *in meso* protein crystallisation. Here, its potential to further tune the curvature of the LCP was investigated.

3.1.6.1. Effect of octyl glucoside. The standard formulation was studied with varying amounts of OG to assess its impact on the Fd3m phase. At low concentrations, the Fd3m structure remained largely unaffected by the addition of OG, as indicated by the presence of well-defined Bragg peaks in the data, Fig. 4A and 4B. However, when the OG concentration reached 5 %, a noticeable disruption in the Fd3m structure was observed where the higher-order peaks became less pronounced. At 10 % OG, only the second peak, which exhibited the highest intensity, remained visible, indicating a significant alteration or potential breakdown of the Fd3m structure.

The phase behaviour of OG alone provides insights into these observations. At 25 °C in water, OG exhibits distinct phase transitions depending on its concentration. At concentrations below 57 wt%, OG forms micelles. As the concentration increases, OG transitions to a mixture of micelles and hexagonal phases at concentrations below 62 wt %, and then to a purely hexagonal phase at concentrations below 65 wt %. Beyond 65 wt%, a combination of hexagonal and cubic phases is observed, with the proportion of OG driving the system towards lower curvature and more continuous structures (Karukstis et al., 2012).

Phase transitions observed in our cases can be attributed to the molecular characteristics of OG, which has a bulky head group and a relatively short hydrophobic chain. These features favour the formation of structures with lower curvature, which could explain the observed disruption of the Fd3m phase at higher OG concentrations. As the OG concentration increases, the system may be driven towards more

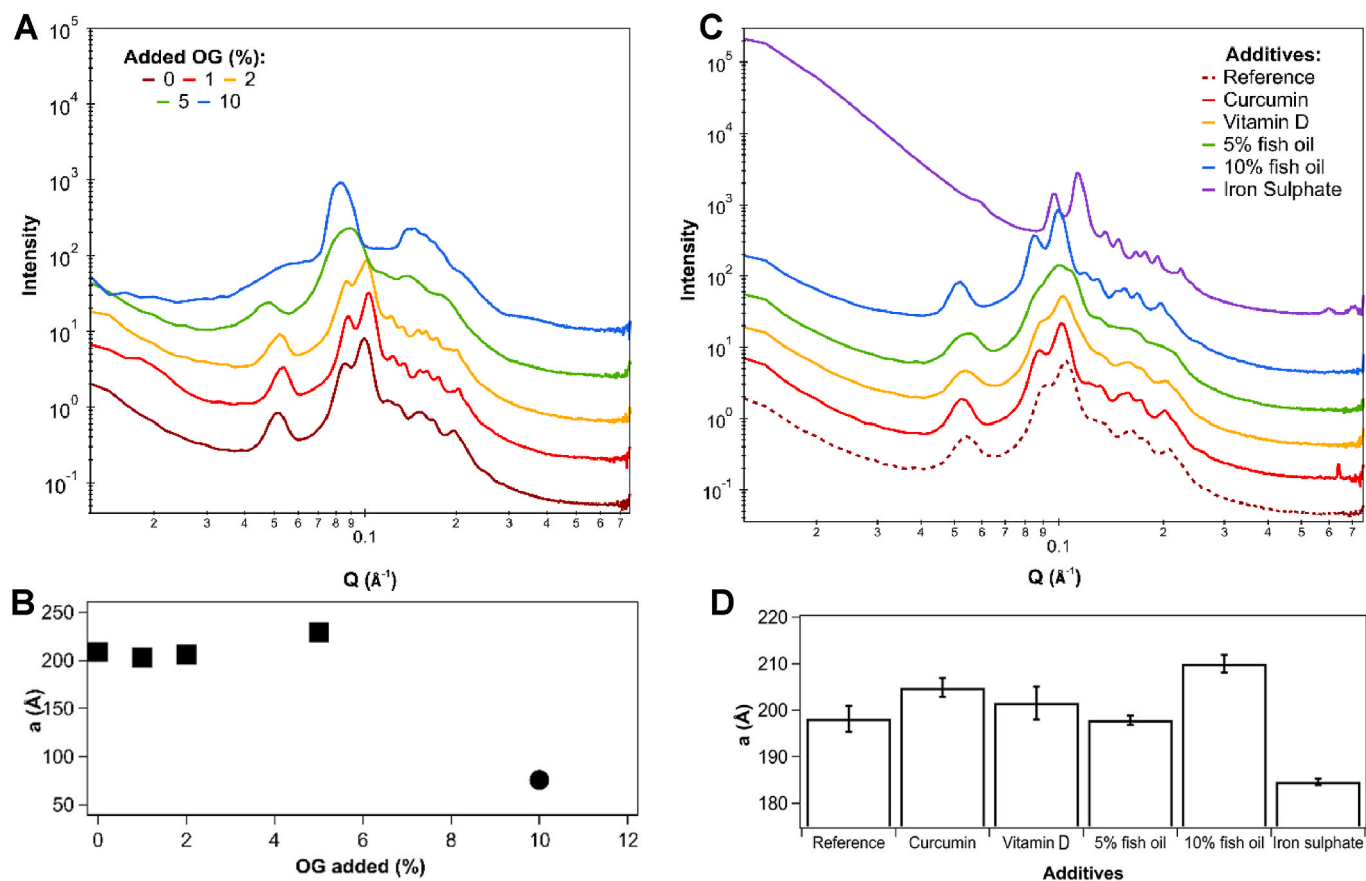


Fig. 4. SAXS data for bulk samples, with a total lipid content of 20 wt%, were prepared using the standard conditions (oat oil with 40 wt% polar lipids (PL40), incubation for 24 h with Lipozyme RM) with curcumin, vitamin D, fish oil, iron sulphate and the OG additives. The effect of increasing proportion of OG (A,B) and doping with selected common nutraceutical additives (C,D) on the lipid liquid crystalline structure was studied. In B, the structure is indicated by the marker shape (disordered/mixed phases = circle, Fd3m micellar cubic = square). All SAXS curves are offset for clarity. Error bars are plotted for all points in B and D. If not visible, they are within the size of the marker.

continuous, less ordered phases, contributing to the loss of higher-order peaks in the SAXS data.

3.1.6.2. Other additives. The data suggests that some tested additives had different effects on the order of the Fd3m structure; changes in lattice parameters were also observed among different additives, Fig. 4C and 4D.

Curcumin: The addition of curcumin resulted in no significant changes to the final Fd3m structure. The SAXS data indicated that the lattice parameter remained stable compared to the reference LCP, suggesting that curcumin does not substantially interact with or disrupt the existing lipid structure in the levels added in this study.

Vitamin D: When vitamin D was incorporated, the Fd3m structure became slightly more disordered. This was evidenced by a broadening of the SAXS peaks, indicating a possible increase in structural heterogeneity. However, the overall phase remained consistent with the baseline Fd3m structure.

Fish Oil: The addition of fish oil produced a minor effect on the Fd3m structure. At a 10 % concentration, the Fd3m phase appeared to become more ordered, with sharper peaks and a lattice parameter more closely aligned with the baseline structure. This suggests that fish oil can be successfully incorporated in the Fd3m structure.

Iron Sulphate: The inclusion of iron sulphate resulted in a noticeable shift to a smaller lattice parameter, accompanied by sharper SAXS peaks. This suggests a more tightly packed or ordered Fd3m structure. Additionally, a low q upturn in the SAXS data was observed. This upturn indicates the formation or presence of larger aggregates or clusters, which is likely due to the iron sulphate either by its effect on the lipid or

due to the presence of iron sulphate particles.

3.2. LCP dispersions

To facilitate further analysis, pre-formed bulk LCPs were collected and subsequently dispersed in a phosphate buffer using the sonication method described in the Methods section. For each dispersion, 50 mg of the LCP was sonicated, resulting in an opaque, white liquid with a viscosity similar to that of water.

The dispersions were prepared to better understand the structural and functional properties of the LCPs in a more fluid state, which is crucial for their potential industrial applications. By dispersing the LCPs, we aimed to determine whether the lipid bulk phase structures remained in the dispersed particle or if they transformed in the presence of a large excess of aqueous buffer and extra energy input of sonication. They transitioned from a bulk, rigid form to a more manageable and adaptable liquid form, which allows for easier handling and manipulation in both experimental and application contexts.

3.2.1. SAXS/WAXS: internal structure of dispersions

3.2.1.1. Incubation time of the bulk phase. None of the dispersion samples without enzyme processing (i.e. oil dispersed in buffer) had any visible peaks in SAXS or WAXS, Fig. S1A,D and Fig. S2A, indicating that the droplets had no ordered internal structure.

In contrast, dispersions prepared from PL40 oat oil, that underwent enzymatic processing with either TL or RM enzymes, displayed a well-defined hexagonal phase. The process of dispersion in excess water by

sonication appeared to facilitate a phase transition from the Fd3m micellar cubic phase to the H_{II} phase. This is characterised by the transformation of discrete micelles into channels arranged on a hexagonal lattice. The excess of water in combination with the sonication process may induce or stabilise the hexagonal arrangement. As these are complex lipid mixture here it cannot be ruled out that the dispersion process might lead to uneven lipid distribution of lipids within the particles.

Interestingly, no significant trends were observed in the SAXS data for the dispersions with respect to incubation time of the corresponding bulk phase for either enzyme, Fig. 5A and 5B. Most samples exhibited similar lattice parameters regardless of the incubation time, Fig. 5C, with the most notable differences occurring at the 2-h mark. For samples incubated for 6 and 24 h, the lattice parameters were remarkably consistent, irrespective of the enzyme used. These results are particularly intriguing given the substantial structural changes observed in the bulk phases over these incubation times. The lack of a corresponding difference in the dispersions raises questions about the factors influencing the structural transitions in dispersed systems versus bulk systems. As discussed above this most likely has to do with the complexity of the lipid mixture. Please note that differences were only observed after 2 h of incubation with the bulk phase. It should also be noted that the lipase is not removed before preparing the dispersion, hence some catalytically active enzyme might have remained in the aqueous phase. Furthermore, the sonication process might have helped to homogenise or stabilise the structures and increase the surface area that can be exposed to the enzyme. These factors might together mask the time-dependent changes that are prominent in bulk samples.

Further analysis using WAXS revealed more pronounced differences, specifically the presence of a crystal peak at $q = 1.44 \text{ \AA}^{-1}$, corresponding to a repeat distance of 4.4 \AA , for samples incubated with Lipozyme TL for 24 h (Fig. S2B) and RM for 6 or 24 h (Fig. S2C). As this peak is only present for the samples which have undergone enzymatic processing, this indicates that the lipolysis induced compositional changes cause this structural change. During incubation, both enzymes hydrolyse TAGs to DAGs, MAGs and FFAs, all of which can form crystal structures depending on the length and saturation of the fatty acid chain (Rogers, 2017, chap. 18). The peak observed in the WAXS data here, agrees well with the expected hydrocarbon chain packing distances for glyceride crystals (Larsson, 1966, 1972).

3.2.1.2. Effect of OG. The effect of increasing OG concentration on the structural properties of the dispersions was also studied. As the OG concentration increased, a noticeable decrease in peak intensity and definition was observed in the SAXS data, Fig. 5E, indicating a reduction in the overall order of the structure, although no significant changes were observed in the WAXS range (Fig. S3). Additionally, with increasing OG levels, there was a small shift to lower q -values, corresponding to an increase in the lattice parameter. At 5 % OG, the SAXS profiles showed no clear peaks, suggesting the complete loss of the hexagonal structure, leading to a disordered structure. This trend parallels the behaviour observed in the bulk phase, where higher concentrations of OG similarly disrupted the ordered Fd3m phase. No distinct trends were identified based on the type of enzyme used, as both TL and RM enzymes exhibited similar behaviours across different OG concentrations. The structural responses to increasing OG percentages were consistent regardless of the enzyme, suggesting that the primary factor influencing the dispersion structure in this context is the concentration of OG rather than the specific enzymatic processing.

3.2.2. CryoTEM: Droplet size and internal structure of LCP dispersions

CryoTEM was employed to further investigate the droplet size, shape and internal structure of the LCP dispersions. The cryoTEM images supported the findings from SAXS and WAXS analysis, revealing that the dispersions consist of nanoparticles (NPs) of varying sizes (50–300 nm),

all of which exhibited a highly ordered internal hexagonal structure, Fig. 6A, B, C. Alongside these NPs, smaller vesicle-like structures of around 10–20 nm were also observed (examples are indicated by red arrows in Fig. 6A), which is common for samples dispersed by sonication.

The high-resolution cryoTEM images clearly displayed the hexagonal lattice within the NPs, providing direct visual confirmation of the internal ordering (Fig. 6B and 6C). The presence of this hexagonal lattice was further validated through Fast Fourier Transform (FFT) analysis, which reinforced the SAXS and WAXS results by highlighting the regularity and periodicity of the internal structures, visible in Fig. S4. These findings are significant as they not only confirm the ordered nature of the NPs seen in SAXS and WAXS but also provide a more detailed visualisation of the nanoscale architecture. The ability to resolve the hexagonal arrangement within the nanoparticles underscores the robust formation of these structures under the given experimental conditions. The presence of smaller vesicle-like entities suggests a possible heterogeneity in the dispersion that could be relevant for their functional applications. This most likely is a consequence of the heterogeneity of the lipid mixture.

3.2.3. Dynamic light scattering: particle size

Dynamic light scattering (DLS) was used to characterise the size distribution of the particles in the dispersions. For the oil samples (i.e. incubation without enzyme), the position of the main peak in the size distribution did not significantly change with incubation time Fig. S6, remaining at $\sim 160 \text{ nm}$. A small peak at large size can be observed for all the distributions, which could correspond to other structures in the system. Here it should be noted that the dynamic light scattering intensity weighted size distribution that overestimates the number of large particles.

For all of the samples which underwent enzymatic processing, high polydispersity and multimodal size distributions were observed, therefore the droplet size distribution was not well-defined.

4. Conclusion

We have demonstrated that the self-assembly structure of natural oat oils, enriched with oat polar lipids, can be controlled by employing lipolytic enzyme processing:

- We developed a novel enzymatic method, which is possible to up-scale, to induce and control the formation of these phases, offering a versatile approach for tailoring the structural properties of lipid-based systems, both in their bulk and dispersed forms. This results in the formation of liquid crystalline phases either in micellar cubic (Fd3m space group) or reverse hexagonal (H_{II}) phase depending on the polar lipid content, either added initially or as a result of lipolytic activity. We have effectively optimised the polar lipid enrichment in the starting material and enzymatic processing conditions (incubation time and choice of enzyme) in order to achieve a stable, highly ordered Fd3m structure in the bulk phase.
- The generated bulk phase can be dispersed into nanoparticles with controllable internal structure that provide fluid systems for delivery of bioactive molecules.
- The effects of various additives, including model dietary supplements and drugs, were systematically tested to assess their impact on the stability and structure of the LCPs and their dispersions. Our findings indicate that while some additives maintain the integrity of the LCPs, others can significantly alter the phase behaviour, particularly at higher concentrations, with implications for both the bulk and dispersed systems.

In conclusion, we have shown that enzymatic processing, combined with careful selection of additives, can effectively modulate the structure and stability of oat oil-based LCPs and their dispersions. These

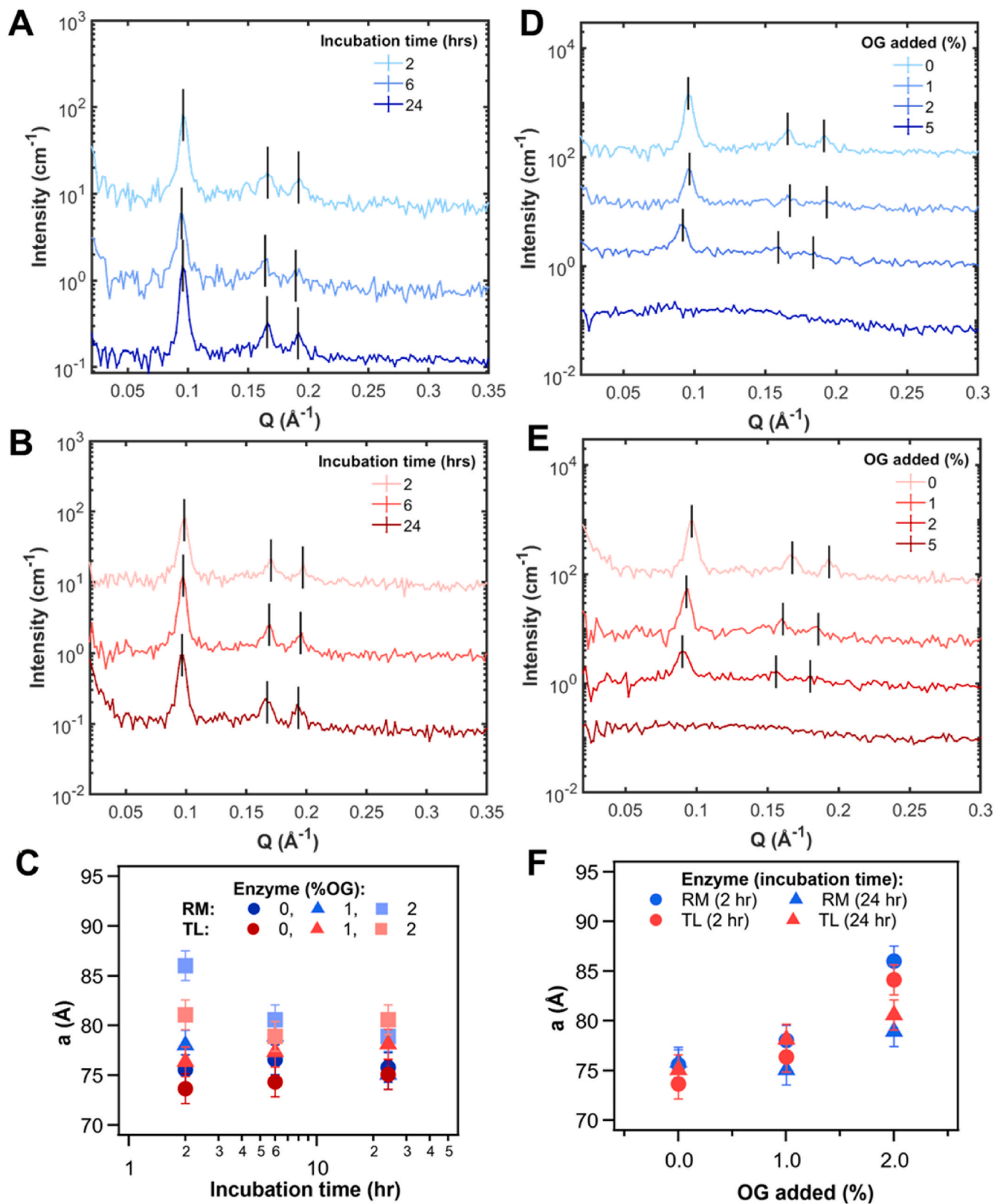


Fig. 5. SAXS data for the dispersion of oat oil sample with 40 wt% polar lipids (PL40) after incubation with Lipzyme TL or RM. Without added OG, incubated with Lipzyme RM or TL for different times are shown in (A) and (B) respectively. The effect of adding OG on the lattice parameters of the samples with different incubation time is shown in (C). It should be noted that the x axis here is on a logarithmic scale. Example SAXS data for the dispersion samples incubated with Lipzyme RM or TL for 24 h with different amounts of added OG are shown in (D) and (E) respectively. The effect of incubation time on the lattice parameters of the samples with different amounts of added OG is shown in (F). All SAXS curves are offset for clarity.

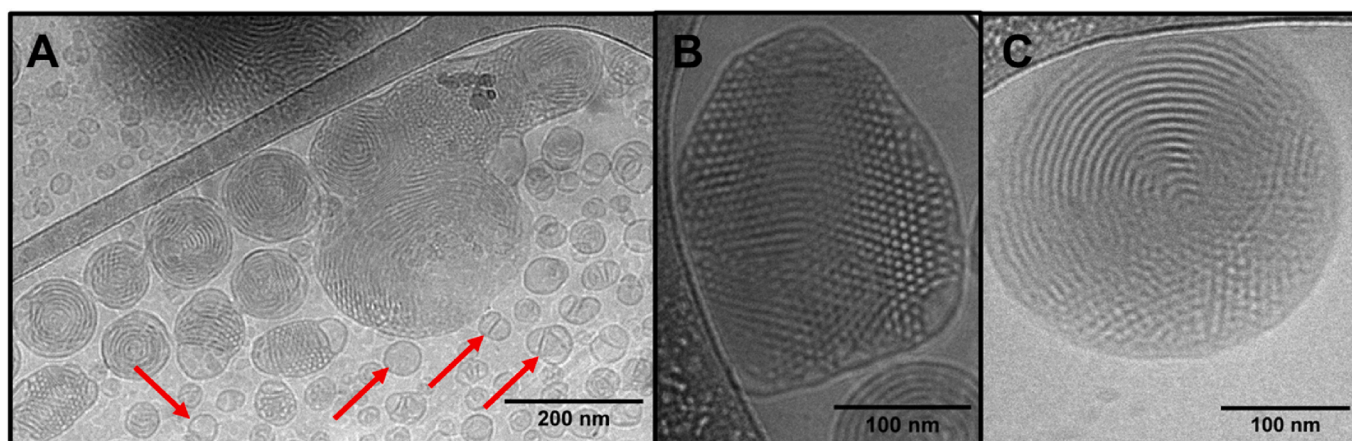


Fig. 6. CryoTEM images of the LCP dispersion (incubation time of 24 h with Lipozyme RM without any additives, 40 % PL oat oil). A mixture of structures present in the dispersion including small vesicle-like structures indicated by red arrows (A), but the sample is dominated by hexosomes (examples highlighted in Fig. 6B and 6C). (For interpretation of the references to colour in this figure legend, the reader is referred to the Web version of this article.)

findings open new avenues for the application of these lipid-based systems in areas such as drug delivery, nutraceuticals, and other industrial formulations. Our research highlights the potential of natural oat oils as a sustainable and functional ingredient in advanced lipid formulations.

CRediT authorship contribution statement

Eimantas Gladkauskas: Writing – original draft, Visualization, Methodology, Investigation, Formal analysis. **Jennifer Gilbert:** Writing – original draft, Visualization, Methodology, Investigation, Formal analysis. **Ben Humphreys:** Writing – review & editing, Visualization, Methodology, Investigation. **Scott Montalvo Diaz:** Writing – review & editing, Methodology, Investigation, Formal analysis. **Anna Maria Piña Cañaveras:** Writing – review & editing, Investigation. **Ann Terry:** Writing – review & editing, Investigation. **Jenny Lindberg Yilmaz:** Writing – review & editing, Methodology, Investigation. **Tommy Nylander:** Writing – review & editing, Supervision, Resources, Funding acquisition, Conceptualization. **Patrick Adlercreutz:** Writing – review & editing, Supervision, Resources, Investigation, Funding acquisition. **Cecilia Tullberg:** Writing – review & editing, Supervision, Methodology, Investigation, Conceptualization.

Declaration of competing interest

The authors declare the following financial interests/personal relationships which may be considered as potential competing interests: Cecilia Tullberg, Patrick Adlercreutz, Tommy Nylander and Eimantas Gladkauskas are shareholders in a spin-off startup Emulsi Biotech AB. The startup explores commercialization potential of the research conducted in this manuscript. Other authors declare no potential competing interests.

Acknowledgements

This work was funded by the Swedish Foundation for Strategic Research (the Industrial Research Center ScanOats, IRC15-0068), as well as The Swedish Agency for Economic and Regional Growth through the European Regional Development Fund (Grant No 20307448), the Skane Region and by FORMAS, grant number 2020-01860.

Oat oil was kindly provided by Swedish Oat Fiber AB, part of Givaudan.

Swedish Research Council and Swedish Foundation for Strategic Research are acknowledged for access to ARTEMI, the Swedish National Infrastructure in Advanced Electron Microscopy (2021-00171 and RIF21-0026).

Special thanks to Crispin Hetherington for work with cryoTEM.

The authors acknowledge the MAX IV Laboratory for beamtime on the CoSAXS beamline under proposal 20211121. Research conducted at MAX IV, a Swedish national user facility, is supported by Vetenskapsrådet (Swedish Research Council, VR) under contract 2018-07152, Vinnova (Swedish Governmental Agency for Innovation Systems) under contract 2018-04969 and Formas under contract 2019-02496.

Appendix A. Supplementary data

Supplementary data to this article can be found online at <https://doi.org/10.1016/j.foodhyd.2025.111378>.

Data availability

Data will be made available on request.

References

- Amara, S., Gerlei, M., Jeandel, C., Sahaka, M., Carrière, F., & Linder, M. (2024). In vitro gastrointestinal digestion of marine oil emulsions and liposomal solutions: Fate of LC-PUFAs upon lipolysis. *Food & Function*, 15, Article 11291. <https://doi.org/10.1039/d4fo03161j>
- Barauskas, J., Johnson, M., & Tiberg, F. (2005). Self-assembled lipid superstructures: Beyond vesicles and liposomes. *Nano Letters*, 5(8), 1615–1619. <https://doi.org/10.1021/nl050678i>
- Barauskas, J., & Landh, T. (2003). Phase behavior of the phytantriol/water system. *Langmuir*, 19(23), 9562–9565. <https://doi.org/10.1021/la0350812>
- Barauskas, J., & Nylander, T. (2008). "Lyotropic liquid crystals as delivery vehicles for food ingredients. *Delivery and controlled release of bioactives in foods and nutraceuticals*. Cambridge: Woodhead Publishing. <https://doi.org/10.1533/9781845694210.1.107>, 107–131.
- Barchan, N., & Adlercreutz, P. (2024). Synthesis of glycopospholipid conjugates with mono- and disaccharides by enzymatic transphosphatidylation. *European Journal of Lipid Science and Technology*, 126, Article e2300240. <https://doi.org/10.1002/ejlt.202300240>
- Barriga, H. M. G., Holme, M. N., & Stevens, M. M. (2019). Cubosomes: The next generation of smart lipid nanoparticles? *Angewandte Chemie International Edition*, 58(10), 2958–2978. <https://doi.org/10.1002/anie.201804067>
- Borné, J., Nylander, T., & Khan, A. (2002). Effect of lipase on different lipid liquid crystalline phases formed by oleic acid based acyl glycerols in aqueous systems. *Langmuir*, 18, 8972–8981. <https://doi.org/10.1021/la020377d>
- Boyd, B. J., Andrew, J., & Clulow, A. J. (2021). The influence of lipid digestion on the fate of orally administered drug delivery vehicles. *Biochemical Society Transactions*, 49, 1749–1761. <https://doi.org/10.1042/BST20210168>
- Costa-Balogh, F. O., Sparr, E., Sousa, J. J. S., & Pais, A. C. (2010). Drug release from lipid liquid crystalline phases: Relation with phase behavior. *Drug Development and Industrial Pharmacy*, 36(4), 470–481. <https://doi.org/10.3109/03639040903261997>
- De Los Reyes, C., Ortega, M. J., Rodríguez-Luna, A., Talero, E., Motilva, V., & Zubia, E. (2016). Molecular characterization and anti-inflammatory activity of galactosylglycerides and galactosylceramides from the microalga *isochrysis galbana*. *Journal of Agricultural and Food Chemistry*, 64, 8783–8794. <https://doi.org/10.1021/acs.jafc.6b03931>

- Doehrlert, D. C., Moreau, R. A., Welti, R., Roth, M. R., & McMullen, M. S. (2010). Polar lipids from oat kernels. *Cereal Chemistry*, 87(5), 467–474. <https://doi.org/10.1094/cchem-04-10-0060>
- Dubackic, M., Liu, Y., Kelley, E. G., Hetherington, C., Haertlein, M., Devos, J. M., Linse, S., Sparr, E., & Olsson, U. (2022). α -Synuclein interaction with lipid bilayer discs. *Langmuir*, 38(33), 10216–10224. <https://doi.org/10.1021/acs.langmuir.2c01368>
- Fay, H., Meeker, S., Cayer-Barrioz, J., Mazuyer, D., Ly, I., Nallet, F., Desbat, B., Douliez, J. P., Ponsinet, V., & Mondain-Monval, O. (2012). Polymorphism of natural fatty acid liquid crystalline phases. *Langmuir*, 272–282. <https://doi.org/10.1021/la203841y>. Epub 2011 Dec 15. PMID: 22118375.
- Freire, R. V. M., & Salentinig, S. (2024). Amphiphilic lipids for food functionality. *Current Opinion in Colloid & Interface Science*, 72, Article 101817. <https://doi.org/10.1016/j.cocis.2024.101817>
- Hossain, M. M., Tovar, J., Cloetens, L., & Nilsson, A. (2023). Inclusion of oat polar lipids in a solid breakfast improves glucose tolerance, triglyceridemia, and gut hormone responses postprandially and after a standardized second meal: A randomized crossover study in healthy subjects. *Nutrients*. <https://doi.org/10.3390/nu15204389>
- Huang, Z., Seddon, J. M., & Templer, R. H. (1996). An inverse micellar Fd3m cubic phase formed by hydrated phosphatidylcholine/fatty alcohol mixtures. *Chemistry and Physics of Lipids*, 82(1), 53–61. [https://doi.org/10.1016/0009-3084\(96\)02558-3](https://doi.org/10.1016/0009-3084(96)02558-3). ISSN 0009-3084.
- Kaimainen, M., Ahvenainen, S., Kaariste, M., et al. (2012). Polar lipid fraction from oat (*Avena sativa*): Characterization and use as an o/w emulsifier. *European Food Research and Technology*, 235, 507–515. <https://doi.org/10.1007/s00217-012-1780-1>
- Karukstis, K. K., Duim, W. C., van Hecke, G. R., & Hara, N. (2012). Biologically relevant lyotropic liquid crystalline phases in mixtures of n-octyl β -D-Glucoside and water. Determination of the phase diagram by fluorescence spectroscopy. *The Journal of Physical Chemistry B*, 116(12), 3816–3822. <https://doi.org/10.1021/jp208097c>
- Kulkarni, C. v., Wachter, W., Iglesias-Salto, G., Engelskirchen, S., & Ahualli, S. (2011). Monoolein: A magic lipid? *Physical Chemistry Chemical Physics*, 13(8), 3004–3021. <https://doi.org/10.1039/C0CP01539C>
- Larsson, K. (1966). Classification of glyceride crystal forms. *Acta Chemica Scandinavica*, 20, 2255–2260. <https://doi.org/10.3891/acta.chem.scand.20-2255>
- Larsson, K. (1972). Molecular arrangement in glycerides. *Fette Seifen Anstrichmittel*, 136–142. <https://doi.org/10.1002/lipi.19720740302>
- Larsson, K. (1989). Cubic lipid-water phases: Structure and biomembrane aspects. *Journal of Physical Chemistry*, 93, 7304–7314. [https://doi.org/10.1016/S0959-440X\(05\)80068-5](https://doi.org/10.1016/S0959-440X(05)80068-5)
- Larsson, K. (2009). Lyotropic liquid crystals and their dispersions relevant in foods. *Current Opinion in Colloid & Interface Science*, 14(1), 16–20. <https://doi.org/10.1016/j.cocis.2008.01.006>. ISSN 1359-0294.
- Liu, M., Zhang, Y., Zhang, H., Hu, B., Wang, L., Qian, H., & Qi, X. (2016). The anti-diabetic activity of oat β -D-glucan in streptozotocin-nicotinamide induced diabetic mice. *International Journal of Biological Macromolecules*, 91, 1170–1176. <https://doi.org/10.1016/j.ijbiomac.2016.06.083>. ISSN 0141-8130.
- Luzzati, V., & Husson, F. (1962). The structure of the liquid-crystalline phase of lipid-water systems. *The Journal of Cell Biology*, 12(2), 207–219. <https://doi.org/10.1083/jcb.12.2.207>
- McClements, D. J., & Jafari, S. M. (2018). Improving emulsion formation, stability and performance using mixed emulsifiers: A review *Advances in Colloid and Interface Science*, 251, 55–79, ISSN 0001-8686 <https://doi.org/10.1016/j.cis.2017.12.001>.
- Mele, S., Söderman, O., Ljusberg-Wahrén, H., Thuresson, K., Monduzzi, M., & Nylander, T. (2018). Phase behavior in the biologically important oleic acid/sodium oleate/water system. *Chemistry and Physics of Lipids*, 211, 30–36. <https://doi.org/10.1016/j.chemphyslip.2017.11.017>
- Meng, L., Shen, G., Zhang, S., Zhou, C., Han, Y., & Wen, R. (2023). New technology for the synthesis of glycerol monooleate. *Journal of Oleo Science*, 72(5), 549–556. <https://doi.org/10.5650/jos.ess22180>. ISSN 1347-3352.
- Milak, S., & Zimmer, A. (2015). Glycerol monooleate liquid crystalline phases used in drug delivery systems. *International Journal of Pharmacy*, 478(2), 569–587. <https://doi.org/10.1016/j.ijpharm.2014.11.072>
- Misquitta, Y., & Caffrey, M. (2003). Detergents destabilize the cubic phase of monoolein: Implications for membrane protein crystallization. *Biophysical Journal*, 85, 3084–3096. [https://doi.org/10.1016/S0006-3495\(03\)74727-4](https://doi.org/10.1016/S0006-3495(03)74727-4)
- Mouloungui, Z., Rakotondrazafy, V., Valentin, R., & Zebib, B. (2009). Synthesis of glycerol 1-monooleate by condensation of oleic acid with glycidol catalyzed by anion-exchange resin in aqueous organic polymorphic system. *Industrial & Engineering Chemistry Research*, 48(15), 6949–6956. <https://doi.org/10.1021/ie900101k>
- Ninham, B. W., Larsson, K., & Lo Nostro, P. (2017). Two sides of the coin. Part 1. Lipid and surfactant self-assembly revisited. *Colloids and Surfaces B: Biointerfaces*, 152, 326–338. <https://doi.org/10.1016/j.colsurfb.2017.01.022>
- Ralla, T., Salminen, H., Edelmann, M., Dawid, C., Hofmann, T., & Weiss, J. (2018). Oat bran extract (*Avena sativa* L.) from food by-product streams as new natural emulsifier. *Food Hydrocolloids*, 81, 253–262. <https://doi.org/10.1016/j.foodhyd.2018.02.035>. ISSN 0268-005X.
- Ramezanpour, M., Schmidt, M. L., Bashe, B. Y. M., Pruijm, J. R., Link, M. L., Cullis, P. R., Harper, P. E., Thewalt, J. L., & Tieleman, D. P. (2020). Structural properties of inverted hexagonal phase: A hybrid computational and experimental approach. *Langmuir*, 36(24), 6668–6680. <https://doi.org/10.1021/acs.langmuir.0c00600>, 23.
- Rogers, R. A. (2017). In M. U. Ahmad (Ed.), *Crystallization of fats and fatty acids in edible oils and structure determination in fatty acids* (pp. 541–559). AOCS Press. <https://doi.org/10.1016/B978-0-12-809521-8.00019-2> (Chapter 18) ISBN 9780128095218.
- Rossetti, F. C., Fantini, M. C. A., Carollo, A. R. H., Tedesco, A. C., & Bentley, M. V. L. B. (2011). Analysis of liquid crystalline nanoparticles by small angle X-ray diffraction: Evaluation of drug and pharmaceutical additives influence on the internal structure. *Journal of Pharmaceutical Sciences*, 100(7), 2849–2857. <https://doi.org/10.1002/jps.22522>. ISSN 0022-3549.
- Schneider, C., Rasband, W., & Eliceiri, K. (2012). NIH image to ImageJ: 25 years of image analysis. *Nature Methods*, 671–675. <https://doi.org/10.1038/nmeth.2089>
- Seddon, J. M., Robins, J. D., Gulik-Krzywicki, T., & Delacroix, H. (2000). Inverse micellar phases of phospholipids and glycolipids. Invited Lecture. *Physical Chemistry Chemical Physics*, 2, 4485–4493. <https://doi.org/10.1039/B004916F>
- Tang, Y., Li, S., Yan, J., Peng, Y., Weng, W., Yao, X., & Xu, B. (2022). Bioactive components and health functions of oat. *Food Reviews International*, 39(7), 4545–4564. <https://doi.org/10.1080/87559129.2022.2029477>
- Wang, J.-b., Liu, X.-r., Liu, S.-q., Mao, R.-x., Hou, C., Zhu, N., Liu, R., Ma, H.-j., & Li, Y. (2019). Hypoglycemic effects of oat oligopeptides in high-calorie diet/STZ-induced diabetic rats. *Molecules*, 24, 558. <https://doi.org/10.3390/molecules24030558>
- Wang, X., Zhang, Y., Gui, S., Huang, J., Cao, J., Li, Z., Li, Q., & Chu, X. (2023). Characterization of lipid-based lyotropic liquid crystal and effects of guest molecules on its microstructure: A systematic review. *AAPS PharmSciTech*, 19(5), 2023–2040. <https://doi.org/10.1208/s12249-018-1069-1>
- Yaghmur, A., Ghayas, S., Jan, H., Kalaycioglu, G. D., & Moghimi, S. M. (2023). Omega-3 fatty acid nanocarriers: Characterization and potential applications. *Current Opinion in Colloid & Interface Science*, 67, Article 101728. <https://doi.org/10.1016/j.cocis.2023.101728>. ISSN 1359-0294.
- Yaghmur, A., & Rappolt, M. (2013). Chapter five - the micellar cubic Fd3m phase: Recent advances in the structural characterization and potential applications. In A. Iglic, & C. v Kulkarni (Eds.), *Advances in planar lipid bilayers and liposomes* (Vol. 18, pp. 111–145). Academic Press. <https://doi.org/10.1016/B978-0-12-411515-6.00005-9>.
- Zheng, J., Liang, Y., Li, J., Lin, S., Zhang, Q., Zuo, K., Zhong, N., & Xu, X. (2023). Enzymatic preparation of mono- and diacylglycerols: A review. *Grain & Oil Science and Technology*, 6(4), 185–205. <https://doi.org/10.1016/j.gaost.2023.10.002>. ISSN 2590-2598.